

Measurement of mutual inductance from frequency dependence of impedance of AC coupled circuit using digital dual-phase lock-in amplifier

Michael J. Schaubert, Seth A. Newman, Lindsey R. Goodman, Itsuko S. Suzuki,* and Masatsugu Suzuki†

Department of Physics, State University of New York at Binghamton, Binghamton, New York 13902-6000

(Dated: June 15, 2006)

We present a simple method to determine the mutual inductance M between two coils in a coupled AC circuit by using a digital dual-phase lock-in amplifier. The frequency dependence of the real and imaginary part is measured as the coupling constant is changed. The mutual inductance ($M = kL$) decreases with increasing the distance d between the centers of coils. We show that the coupling constant is proportional to d^{-n} with an exponent n (≈ 3). When the current flows in the coils, the coil is magnetically regarded as the magnetic moment. The physics of the mutual inductance is similar to that of two magnetic moments coupled by a dipole-dipole interaction.

PACS numbers: 01.50.Pa, 01.50.Qb, 01.40.Fk

I. INTRODUCTION

Faraday's law of magnetic induction states that a changing magnetic flux through a coil of wire with respect to time will induce an electromagnetic force (EMF) in the wire.¹ When two separate circuits can exchange energy by means of magnetic induction, they are "coupled." In a coupled circuit, there are two coils of wire; a primary coil that is connected in series with the voltage source, and a secondary coil that is not connected to any voltage source. The secondary coil receives energy only by induction. In a transformer for example, energy is transferred from one circuit to another by means of magnetic coupling alone; the two circuits are not physically connected by any wires. The EMF in the secondary coil affects the total voltage output of the coupled circuit due to reflected impedance. Therefore changing the mutual inductance has an affect on the total voltage output.

The original AC coupled measurement is one of the experiments in the Junior laboratory (undergraduate course) in the Physics Department of our University. Students spend a lot of time in measuring the frequency dependence of the real part of output voltage when the distance between two coils is varied. In spite of their considerable works, we find that students have some difficulty in getting well-defined data and reasonable conclusions. We realize that it is much easier for students to get good data with the use of a digital dual-phase lock-in amplifier (Stanford Research System, SR850).² It has the ability to measure simultaneously the in-phase and out-of phase signal.

Here we present a simple method to measure the frequency dependence of the real part and imaginary part of the output voltage across a resistance in the primary circuit in the coupled AC circuit. The change in distance of two coils facing each other leads to the change of the mutual inductance. The present method allows one to obtain a great deal of data in a reasonably short period of time. Also, previously undeterminable features of the circuit become available when it is combined with the lock-in amplifier. A background for the AC analysis of

the AC coupled circuit in the frequency domain is presented in Sec. III. The frequency dependence of the real part and imaginary part of output voltage is formulated and is simulated using the Mathematica. Our results are reported in Sec. IV. The mutual inductance is determined as a function of the distance between the centers of two coils from the frequency dependence of the real and imaginary parts. We show that the mutual inductance changes with the distance d as d^{-n} where $n \approx 3$. We show that the physics of the mutual inductance is the same as that of magnetic moments which are coupled by a dipole-dipole interaction.

II. EXPERIMENTAL PROCEDURE

The AC coupled circuit in the frequency domain was configured in Fig. 1(a). An AC voltage was sent into the circuit, $v_s(t) = \text{Re}[\tilde{E}e^{j\omega t}]$, where $j = \sqrt{-1}$, \tilde{E} is the complex voltage source, and ω ($= 2\pi f$) is the angular frequency. Two LCR circuits are placed together with inductors, resistors and capacitors attempting to be equivalent ($L_1 = L_2 = 0.821$ H, $R_1 = R_2 = 97$ Ω , and $C = 0.0038$ μF), where the resistance of each coil is 66.0 Ω . The resonance frequency f_0 is equal to $f_0 = 1/(2\pi\sqrt{LC}) = 2850$ Hz. In Fig. 1(b) we show the overview of two coils used in the present measurement. Each coil (Heath Company Part No. 40-694) has a cylindrical form with the inner diameter (9.30 cm), the outer diameter (12.5 cm), and the length (9.0 cm). The number of turns of the coil is $N = 3400$. The minimum distance between the centers of the coils is $d_c = 10.2$ cm. The total distance is $d = d_c + d_s$, where d_s is the separation distance between the edges of the two coils. The two inductors are placed on a meter long track.

A digital dual-phase lock-in amplifier (Stanford SR850) was used to find the real part (μ) and imaginary part (ν) of the output voltage across the resistance (AG) in Fig. 1(a)

$$\begin{aligned} V_{out}(t) &= \text{Re}[(\mu + j\nu)E_0 \exp[j(\omega t + \phi_0)]] \\ &= E_0\mu \cos(\omega t + \phi_0) + E_0\nu \cos(\omega t + \phi_0 + \pi/2). \end{aligned}$$

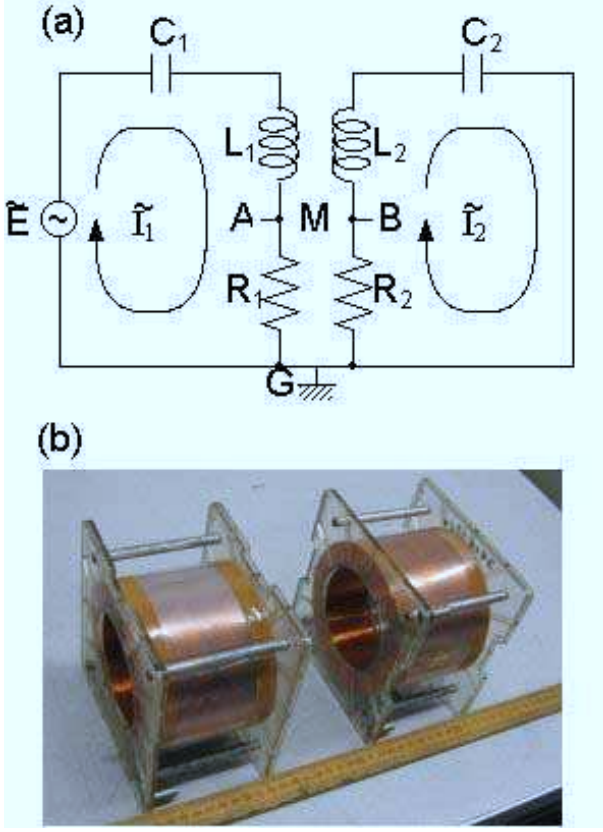


FIG. 1: (Color online) (a) AC coupled circuit used in the present experiment. The primary circuit is on the left side, the secondary circuit on the right side. The coils 1 and 2 are used in place of the inductors L_1 and L_2 . The resistances (R_1 and R_2) and the capacitances (C_1 and C_2) are fixed. An AC voltage was supplied by the lock-in amplifier. (b) A picture of two coils used in the measurement.

(1)

where $\tilde{E} = E_0 e^{j\phi_0}$ and ϕ_0 is the phase. The in-phase component of the lock-in amplifier is equal to $E_0\mu$ and the out-of phase component is equal to $E_0\nu$, where $E_0 = 4.97$ mV. So one can determine the values of real part μ and imaginary part ν of the output voltage, independently. The digital dual-phase lock-in amplifier has a frequency sweep feature so that it will measure across a certain frequency range. The measurements are repeated for numerous distances ranging from 10.2 cm to 70.2 cm. The frequency range initially is 2500 Hz to 3500 Hz, but after 25.2 cm separation the frequency scan is only needed to be across 2700 Hz - 3000 Hz.

III. BACKGROUND

A. Mutual inductance

For simplicity, we assume that each coil has a cylindrical form with a radius R_{av} and a length l . The separation

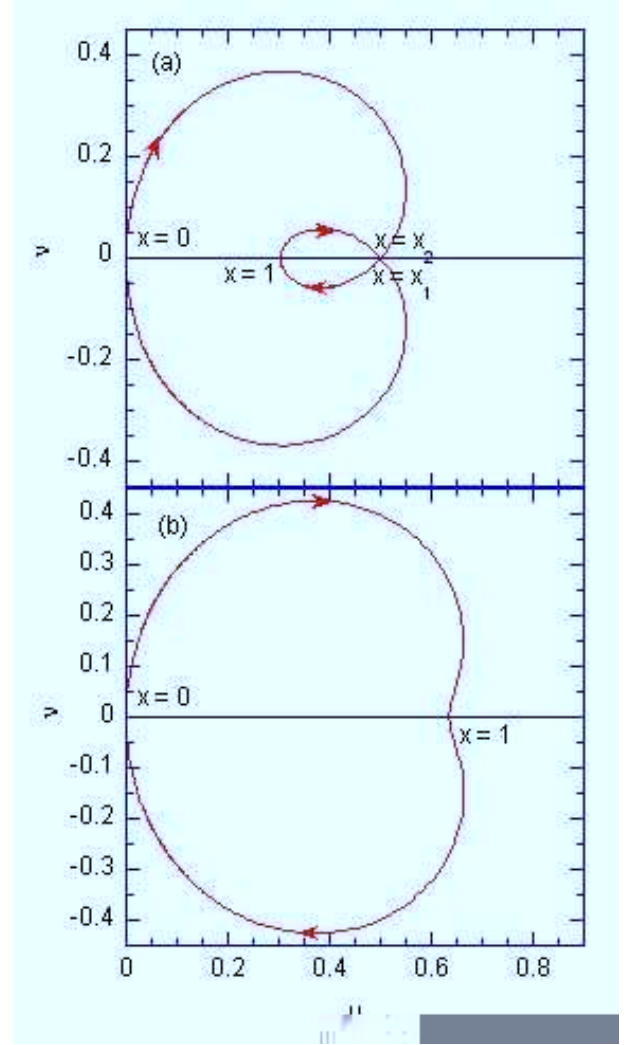


FIG. 2: (Color online) (a) The state-1. Simulation plot of the trajectory denoted by the point (μ, ν) for $kQ > 1$ and $L_1 = L_2$ (the symmetric configuration), when $x (= f/f_0)$ varies from $x = 0$ to ∞ . The figure corresponds to the case of $kQ = 1.515$ where $Q = 151.5$ and $k = 0.01$. The point on the trajectory is located at the origin ($\mu = 0$ and $\nu = 0$) at $x = 0$, at $\mu = 1/2$ and $\nu = 0$ at $x = x_2$, $\mu = 1/[1 + (kQ)^2]$ ($< 1/2$) and $\nu = 0$ at $x = 1$, at $\mu = 1/2$ and $\nu = 0$ at $x = x_1$, and at the origin at $x = \infty$. (b) The state-2. Simulation plot of the trajectory denoted by the point (μ, ν) for $kQ < 1$, when x varies from $x = 0$ to ∞ . The figure corresponds to the case of $kQ = 0.7575$ where $Q = 151.5$ and $k = 0.005$. The point is located at the origin ($\mu = 0$ and $\nu = 0$) at $x = 0$, $\mu = 1/[1 + (kQ)^2]$ ($> 1/2$) and $\nu = 0$ at $x = 1$, and at the origin at $x = \infty$.

between the centers of two coils (see Fig. 1(b)) is the distance d . The number of turns of the coils 1 and 2 is the same (N). The magnetic field produced by coil 1 (current I_1) at the center of coil 2 is given by

$$B = \frac{\mu_0}{2\pi} \frac{NA}{d^3} I_1, \quad (2)$$

for $d \gg R_{av}$ using the Bio-Savart law. The voltage induced in the coil 2 is

$$V_2 = -N \frac{d\Phi}{dt} = -NA \frac{dB}{dt} = -\frac{\mu_0 N^2 A^2}{2\pi d^3} \frac{dI_1}{dt}, \quad (3)$$

where the magnetic flux is $\Phi = BA$ and A is the cross-sectional area of the solenoid: $A = \pi R_{av}^2$. Thus the mutual inductance M defined by $V_2 = -M dI_1/dt$ is given by

$$M = \frac{\mu_0 N^2 A^2}{2\pi d^3}. \quad (4)$$

The self-inductance L is given by

$$L = \frac{\mu_0 N^2 A}{l}, \quad (5)$$

where l is the length of solenoid, $\mu_0 (= 4\pi \times 10^{-7} \text{ Tm/A})$ is a permeability, and N is the total number of turn. Thus we have

$$k = \frac{Al}{2\pi d^3} = \frac{R_{av}^2 l}{2d^3}, \quad (6)$$

since $M = kL$. The constant k is dependent only on the geometry of the coils. Note that our coils used in the present measurement has $N = 3400$ turn and $l = 10.2$ cm. When $R_{av} = 5.45$ cm, and $l = 10.2$ cm, we have $R_{av}^2 l / 2 = 151.5$, where d is in the units of cm. The self-inductance L_{cal} can be calculated as

$$L_{cal} = \frac{\mu_0 N^2 \pi R_{av}^2}{l} = 1.329 \text{ H}.$$

This value of L_{cal} is a little larger than the actual value of L_{exp} ($= 0.821$ H). The difference between L_{exp} and L_{cal} is due to the deviation of the system from ideal one: $L_{exp} = K L_{cal}$, where K is called the Nagaoka coefficient.³ The value of K is nearly equal to 0.67 for the ratio $2R/l = 2 \times 5.45/10.2 \approx 1.07$

B. AC couple circuit

In Fig. 1(a) we show the AC coupled circuit in the frequency domain.⁴ The currents and voltages are all complex number. Using the Kirchhoff's law, we can write down two equations,

$$\tilde{E} = \tilde{I}_1 Z_1 + j\omega M \tilde{I}_2, \quad (7)$$

and

$$0 = \tilde{I}_2 Z_2 + j\omega M \tilde{I}_1,$$

or

$$\tilde{I}_2 = -\frac{j\omega M \tilde{I}_1}{Z_2}, \quad (8)$$

where \tilde{I}_1 and \tilde{I}_2 are the loop currents of the primary and secondary circuit, \tilde{E} is the source voltage, Z_1 and Z_2 are the impedance of the primary and secondary circuits, respectively,

$$Z_1 = R_1 + jX_1, (X_1 = \omega L_1 - \frac{1}{\omega C_1}),$$

$$Z_2 = R_2 + jX_2, (X_2 = \omega L_2 - \frac{1}{\omega C_2}),$$

without the coupling between the primary and secondary circuits and M is the mutual inductance and is dependent on the distance between the self inductances of L_1 and L_2 . Then we have

$$\tilde{E} = \tilde{I}_1 Z_1 + j\omega M (-\frac{j\omega M \tilde{I}_1}{Z_2}), \quad (9)$$

or

$$\tilde{E} = Z'_1 \tilde{I}_1,$$

where Z'_1 is the effective impedance of the primary circuit and is defined as

$$Z'_1 = \frac{\tilde{E}}{\tilde{I}_1} = Z_1 + \frac{\omega^2 M^2}{Z_2}.$$

The primary impedance is rewritten as

$$Z'_1 = R'_1 + jX'_1 = R_1 + \frac{\omega^2 M^2 R_2}{R_2^2 + X_2^2} + j(X_1 - \frac{\omega^2 M^2 X_2}{R_2^2 + X_2^2}).$$

For simplicity, we assume the symmetric configuration such that $R_1 = R_2 = R$, $C_1 = C_2 = C$, and $L_1 = L_2 = L$. Then we have $X = X_1 = X_2 = \omega L - 1/\omega C$. The impedance Z'_1 can be written as

$$Z'_1 = R + \frac{\omega^2 M^2 R}{R^2 + X^2} + j(X - \frac{\omega^2 M^2 X}{R^2 + X^2}).$$

The voltage across R_1 ($= R$) between AG in Fig. 1(a) \tilde{V}_R is

$$\tilde{V}_R = \tilde{I}_1 R = \tilde{G} \tilde{E},$$

where

$$\tilde{G} = \frac{R}{R(1 + \frac{\omega^2 M^2}{R^2 + X^2}) + jX(1 - \frac{\omega^2 M^2}{R^2 + X^2})}. \quad (10)$$

We define the ratio as $x = \omega/\omega_0$, where $\omega_0 = 1/\sqrt{LC}$ and x is always positive. The quality factor of the circuit is defined by

$$Q = \frac{\omega_0 L}{R} = \frac{1}{R} \sqrt{\frac{L}{C}}. \quad (11)$$

The mutual inductance M is related to the self inductance L by

$$M = k \sqrt{L_1 L_2} = kL, \quad (12)$$

where k is a constant and is smaller than 1. Then \tilde{G} is rewritten as

$$\begin{aligned}\tilde{G} &= \mu + j\nu \\ &= \frac{x[x + jQ(x^2 - 1)]}{x^2 + 2jQx(x^2 - 1) + Q^2[2x^2 - 1 + (k^2 - 1)x^4]},\end{aligned}$$

which depends only on x , Q , and k . The real part of \tilde{G} ($= \mu$) is given by

$$\mu = \frac{x^2[Q^2(1 + k^2)x^4 + (1 - 2Q^2)x^2 + Q^2]}{x^4 + Q^4[(k^2 - 1)x^4 + 2x^2 - 1]^2 + 2Q^2[(1 + k^2)x^6 - 2x^4 + x^2]}.$$

The imaginary part of \tilde{G} ($= \nu$) is

$$\nu = \frac{-Qx(x + 1)(x - 1)[Q^2(1 - k^2)x^4 + (1 - 2Q^2)x^2 + Q^2]}{x^4 + Q^4[(k^2 - 1)x^4 + 2x^2 - 1]^2 + 2Q^2[(1 + k^2)x^6 - 2x^4 + x^2]}.$$

Note that ν becomes zero at least at $x = 0$ and 1. We now consider only the case of $k < 1$ and $Q \gg 1$, which corresponds to the present experiment. For convenience we consider the quadratic equation

$$g(t) = Q^2(1 - k^2)x^4 + (1 - 2Q^2)x^2 + Q^2 = 0. \quad (16)$$

The solution of this equation is formally given by

$$x_1 = \sqrt{\frac{2Q^2 - 1 + \sqrt{1 - 4Q^2 + 4k^2Q^4}}{2(1 - k^2)Q^2}}, \quad (17)$$

and

$$x_2 = \sqrt{\frac{2Q^2 - 1 - \sqrt{1 - 4Q^2 + 4k^2Q^4}}{2(1 - k^2)Q^2}}, \quad (18)$$

where

$$x_1 x_2 = \frac{1}{\sqrt{1 - k^2}}, \quad (19)$$

and

$$x_1^2 - x_2^2 = \frac{\sqrt{1 - 4Q^2 + 4k^2Q^4}}{Q^2(1 - k^2)}.$$

Here we have $\mu = 1/2$, $\nu = 0$ at $x = x_1$, $\mu = 1/(1 + k^2Q^2)$, $\nu = 0$ at $x = 1$, $\mu = 0$, $\nu = 0$ at $x = 0$, and $\mu = 0$, $\nu = 0$ at $x = \infty$.

(1) The state-I for $4Q^2(k^2Q^2 - 1) + 1 > 0$. This condition is nearly equivalent to $kQ > 1$ since $Q \gg 1$. There are two solutions x_1 and x_2 ($0 < x_2 < 1 < x_1$) besides $x = 0$ and 1. In Fig. 2(a) we show the simulation plot of the trajectory of the point (μ, ν) for $kQ > 1$ and

$L_1 = L_2$ (the symmetric configuration), when x varies from $x = 0$ to ∞ . This figure corresponds to the case of $kQ = 1.515$ where $Q = 151.5$ and $k = 0.01$.

(2) The state-II for $4Q^2(k^2Q^2 - 1) + 1 < 0$. This condition is nearly equivalent to $kQ < 1$. There is no solution, besides $x = 0$ and 1. In Fig. 2(b) we show the simulation plot of the trajectory of the point (μ, ν) for $kQ < 1$ and $L_1 = L_2$ (the symmetric configuration), when x varies from $x = 0$ to ∞ . This figure corresponds to the case of $kQ = 0.758$, where $Q = 151.5$ and $k = 0.005$.

Numerical calculations of μ and ν were made using the Mathematica program. Figures 3(a) and (b) show simulated plots of the real part (μ) and the imaginary part (ν) as a function of x , where $Q = 151.5$ and $L_1 = L_2$ (symmetric configuration). The coupling constant k is changed as a parameter: $k = 0 - 0.1$. In Fig. 3(a), the double peaks in the μ vs x curve are symmetric with respect to $x = 1$ and becomes closer and closer together as k is decreased and becomes a single peak at $kQ \approx 0.5757$. The imaginary part ν (see Fig. 3(b)) has a positive local minimum at $x = 0.9967$ and a negative local maximum at $x = 1.0033$ in the limit of $k \rightarrow 0$. Figure 3(c) shows the trajectory denoted by the point (μ, ν) for $Q = 151.5$ and $L_1 = L_2$ (the symmetric configuration), when x is varied from $x = 0$ to ∞ . The coupling constant k is changed as a parameter: $k = 0 - 0.1$. There is a drastic change of the trajectory from the state-I and state-II at $kQ = 1$, when kQ is decreased. For $k = 0$, the trajectory is a circle of radius $1/2$ centered at $\mu = 1/2$ and $\nu = 0$.

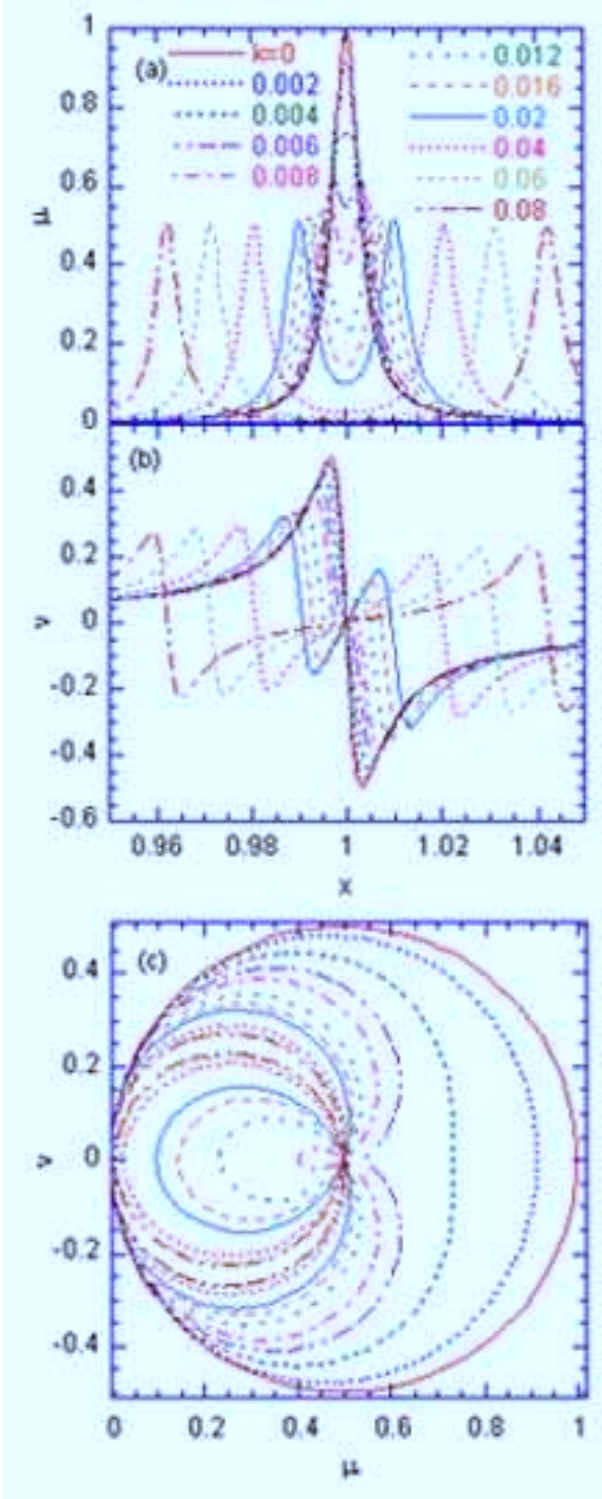


FIG. 3: (Color online) Simulation plot of (a) the real part (μ) and (b) the imaginary part (ν) as a function of x (calculations), where $Q = 151.5$ and $L_1 = L_2$ (symmetrical case). The parameter k is changed as a parameter: $k = 0 - 0.1$. (c) Typical trajectory denoted by the point (μ, ν) for $Q = 151.5$ and $L_1 = L_2$ (the symmetric configuration), when x is varied from $x = 0$ to ∞ . The parameter k is changes as a parameter: $k = 0 - 0.1$.

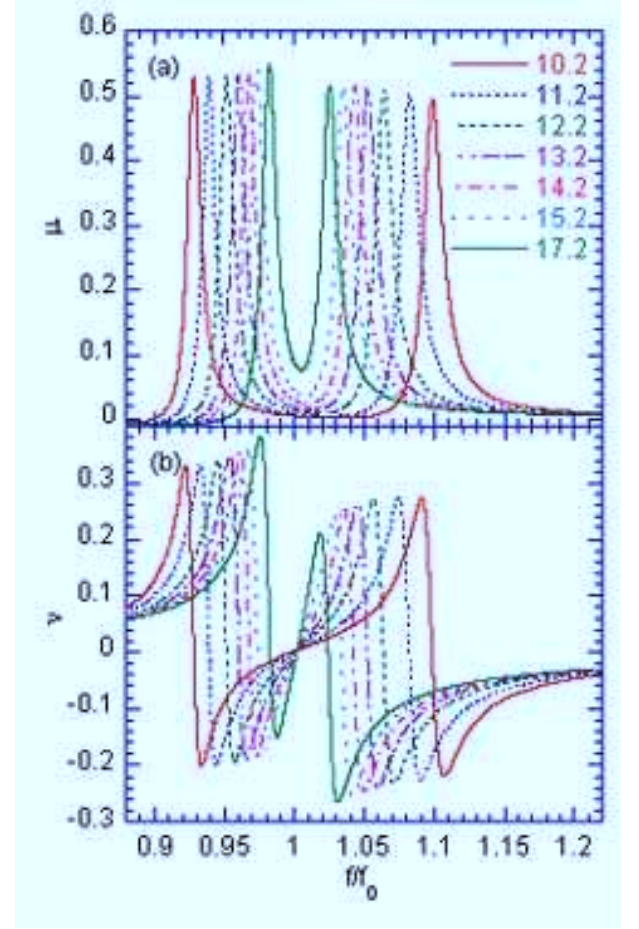


FIG. 4: (Color online) Experimental plot of (a) the real part (μ) and (b) the imaginary part (ν) as a function of $x (= f/f_0)$ (in the frequency scan). The distance d between the centers of two coils is changed as a parameter. $d = 10.2$ cm - 17.2 cm. where $f_0 = 2850$ Hz. $Q = 151.5$.

IV. RESULT

We have measured the frequency dependence of the real part μ and the imaginary part ν when the distance d between the centers of two coils is changed as a parameter: $d = 10.2 - 70.2$ cm. Our results are shown in Figs. 4 - 6. Figures 4 and 5 shows the experimental plot of the real part (μ) and the imaginary part (ν) as a function of $x (= f/f_0)$, where $f_0 = 2850$ Hz and $Q = 151.5$. In Figs. 4(a) and (b) double peaks of μ becomes closer and closer when d is increased and the double peaks becomes a single peak around $d = 36.2$ cm. The double peaks are not symmetric with respect $x = 1$. The peak at the lower- x side is higher than that at the higher- x side. The real part has a local minimum at x which is a little larger than 1. In Fig. 5(a) and (b) the imaginary part ν crosses the $\nu = 0$ line at $x = x_2$, $x \approx 1$, and $x = x_1$ ($> x_2$). The positions x_1 and x_2 becomes closer and closer as d is decreased and combines into the position $x \approx 1$, but not at $x = 1$. Figure 6 shows the experimental trajectory

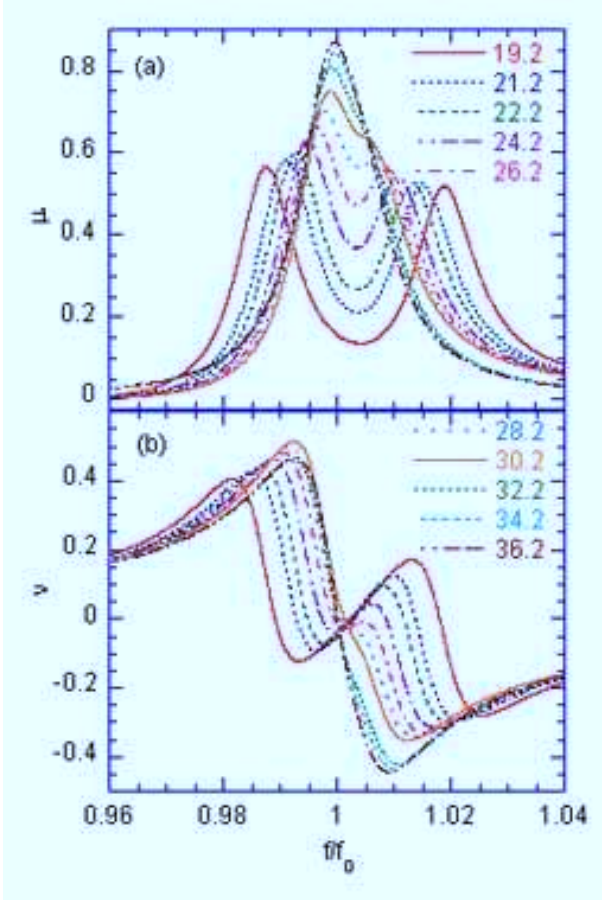


FIG. 5: (Color online) Experimental plot of (a) the real part (μ) and (b) the imaginary part (ν) as a function of x ($= f/f_0$) (in the frequency scan). The distance d between the centers of two coils is changed as a parameter. $d = 19.2$ cm - 36.2 cm. where $f_0 = 2850$ Hz. $Q = 151.5$.

ries of the point (μ, ν) for $Q = 151.5$, when x ($= f/f_0$) is varied from $x = 0.947$ ($f = 2700$ Hz) to 1.053 ($f = 3000$ Hz), and $f_0 = 2850$ Hz. The distance d is changed as a parameter: $d = 13.2$ - 36.2 cm. The transition occurs between the state-I and state-II at $d \approx 27.2$ cm. The overview of our trajectory is similar to the simulation plot as shown in Fig. 3(c). However our trajectory rotates clockwise compared to the ideal simulation plot (the symmetric configuration). The deviation of our trajectories from the ideal case (Fig. 3(c)) is partly due to the asymmetric configuration (L_1 is slightly larger than L_2).

Figure 7(a) shows the zero-crossing frequencies normalized by f_0 for the imaginary part (ν) (at which ν becomes zero) as a function of the distance d (cm), where $x_2 = f_2/f_0$ (< 1), $x_c = f_c/f_0$ (≈ 1), $x_1 = f_1/f_0$ (> 1), and $f_0 = 2850$ Hz. The value of x_c is a little different from 1. In Fig. 7(a) we also show the normalized frequency defined by $(x_1 x_2)^{1/2}$. This frequency decreases with increasing d . This implies that the parameter k decreases with increasing d , since $(x_1 x_2)^{1/2} = (1 - k^2)^{-1/4}$

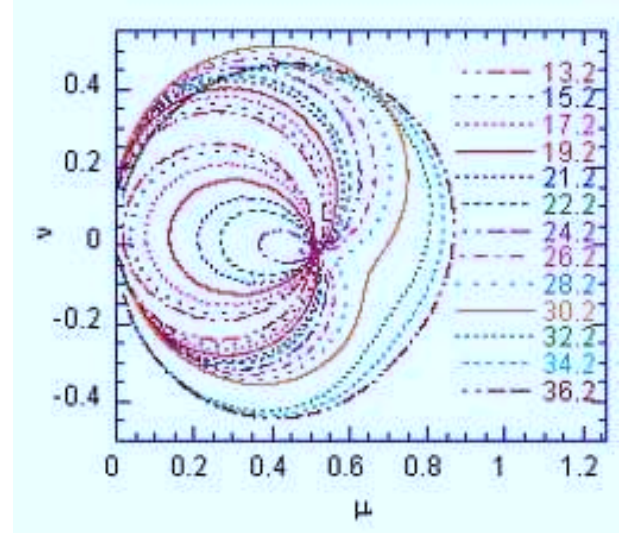


FIG. 6: (Color online) Experimental trajectories of the point (μ, ν) for $Q = 151.5$, when x ($= f/f_0$) is varied from $x = 0.947$ ($f = 2700$ Hz) to 1.053 ($f = 3000$ Hz), and $f_0 = 2850$ Hz. The distance is changed as a parameter: $d = 13.2$ - 36.2 cm. The deviation of the experimental trajectories from the ideal one as shown in Fig. 3(c) is partly due to the asymmetric configuration (L_1 is slightly larger than L_2).

which is predicted from Eq.(19).

Figure 7(b) shows the normalized peak frequencies of the real part (μ) as a function of the distance d (cm), where $x_d = f_d/f_0$ (< 1), $x_u = f_u/f_0$ (> 1), and $f_0 = 2850$ Hz. The real part μ takes double peaks at the lower and upper frequencies f_d and f_u for $d < 30$ cm. The d dependence of x_u and x_d is similar to that of x_1 and x_2 , respectively. In Fig. 7(b) we also show the normalized frequency defined by $(x_u x_d)^{1/2}$ as a function of d . This frequency decreases with increasing d like $(x_1 x_2)^{1/2}$ in Fig. 7(a).

V. DISCUSSION

First we show that from a view point of physics, the AC coupled circuit with the mutual inductance is equivalent to the magnetic moments \tilde{M}_1 ($= \mu_0 N I_1 A$) for the coil 1 and \tilde{M}_2 ($= \mu_0 N I_2 A$) for the coil 2. They are coupled with a dipole-dipole interaction defined by

$$U_{12} = \frac{1}{4\pi\mu_0} \left[\frac{\tilde{M}_1 \cdot \tilde{M}_2}{r^3} - \frac{3(\tilde{M}_1 \cdot \mathbf{r})(\tilde{M}_2 \cdot \mathbf{r})}{r^5} \right], \quad (20)$$

where \mathbf{r} is the position vector connecting between the centers of coils 1 and 2. When both \tilde{M}_1 and \tilde{M}_2 are parallel to the direction of \mathbf{r} , a ferromagnetic arrangement of two magnetic moments is energetically favorable,

$$\tilde{U}_{12} = -\frac{2}{4\pi\mu_0} \frac{\tilde{M}_1 \tilde{M}_2}{d^3} = -\frac{\mu_0^2 N^2 A^2}{2\pi\mu_0 d^3} I_1 I_2. \quad (21)$$

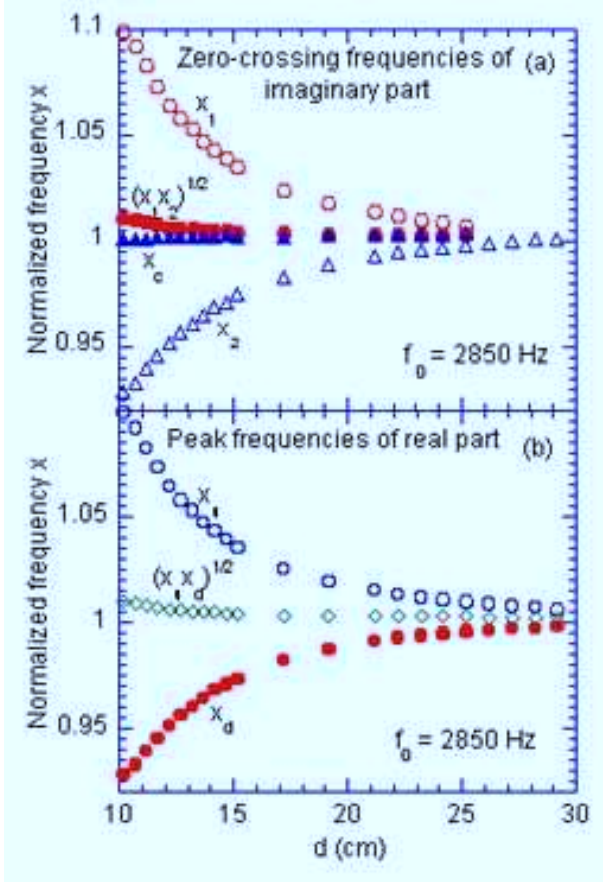


FIG. 7: (Color online) The Normalized zero-crossing frequencies of the imaginary part (ν) (at which ν becomes zero) as a function of the distance d (cm). $x_2 = f_2/f_0$ (< 1), $x_c = f_c/f_0$ (≈ 1), $x_1 = f_1/f_0$ (> 1), and $f_0 = 2850$ Hz. The normalized frequency defined by $(x_1 x_2)^{1/2}$ is also shown for comparison. (b) The Normalized peak frequencies of the real part (μ) as a function of the distance d (cm). $x_d = f_d/f_0$ (< 1) and $x_u = f_u/f_0$ (> 1). $f_0 = 2850$ Hz. The real part μ takes two peaks at the lower and upper frequencies f_d and f_u for $d < 30$ cm. The normalized frequency defined by $(x_u x_d)^{1/2}$ is also shown for comparison.

From the definition of the mutual inductance M , the interaction energy \tilde{U}_{12} can be described by $\tilde{U}_{12} = -MI_1 I_2$, leading to the mutual inductance which is the same as Eq.(4) derived from the Faraday's law.

It is predicted that the parameter k changes with the distance d according to Eq.(6); k is proportional to d^{-3} . The first method to determine the parameter k as a function of the distance d , is as follows. As shown in Sec. III, it is predicted that in the symmetrical configuration ($L_1 = L_2 = L$), the real part μ takes a $\mu = 1/[1 + (kQ)^2]$ at $x = 1$. Note that the imaginary part ν is equal to zero at $x = 1$. Experimentally we have determined the value of μ at $x = 1$ as a function of d . The values of k are derived from the above expression with $Q = 151.5$. Figure 8(a) shows the plot of k vs d thus obtained. The value of k drastically decreases with increasing d and almost

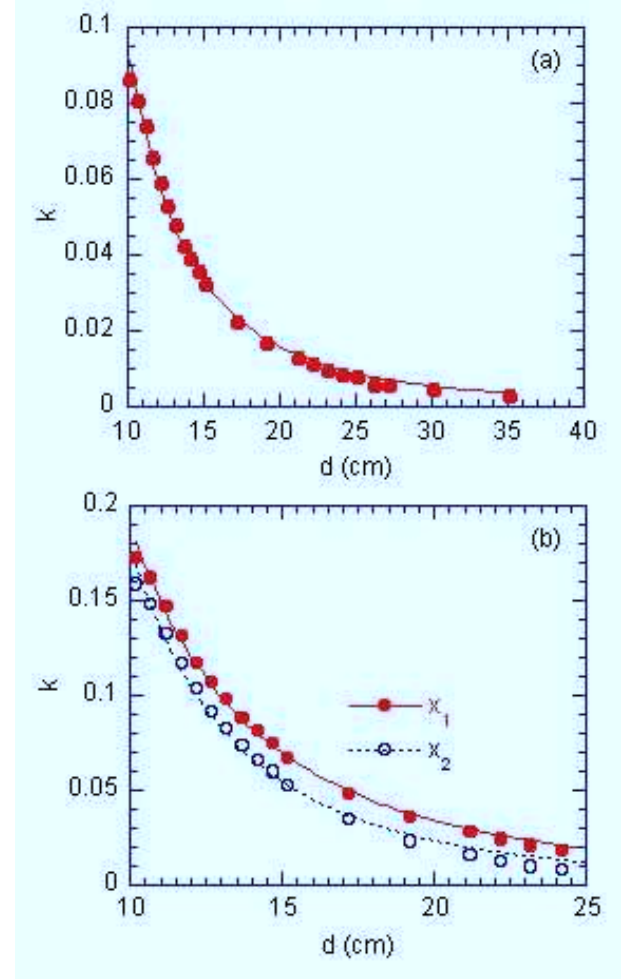


FIG. 8: (Color online) (a) and (b) Plot of k as a function of the distance d . $Q = 151.5$. (a) The value of k is derived from the prediction that the real part (μ) is equal to $1/[1 + (kQ)^2]$ at $x = 1$ for the symmetrical configuration ($L_1 = L_2$). The best fitted curve to the expression given by Eq.(22) is denoted by a solid line. (b) The values of k are derived from the prediction that x_1 and x_2 are described by Eqs.(17) and (18). The values of k are numerically solved for each d . The best fitted curves are shown by the dotted and solid lines in the figure.

reduces to zero at $d = 35$ cm. The least-squares fit of the data of k vs d to an expression

$$k = \frac{\zeta}{d^n}, \quad (22)$$

yields a constant $\zeta = 38.5 \pm 5.0$ and the exponent $n = 2.60 \pm 0.05$, where d is in the units of cm. The value of ζ is rather different from the predicted value for the present coils ($\zeta = 151.5$), while the value of n is rather close to the predicted value ($n = 3$). The large deviation of the experimental value of ζ from our prediction may be related to the asymmetric configuration of L_1 and L_2 in the present system, where L_2 is slightly lower than L_1 (which will be discussed later). As shown in Fig. 4(a), the value of x where the real part μ has a local minimum

is not equal to $x = 1$, and shifts to the high- x side.

The second method to determine the value of k is as follows. In Sec. III, it is predicted that the imaginary part ν takes zero-crossing at $x = x_2$, 1, and x_1 in the case of the symmetrical configuration ($L_1 = L_2 = L$). Note that the imaginary part ν is not always equal to zero at $x = 1$ partly because of the asymmetric configuration in the present experiment. The value of k for each d is derived by applying the Mathematica program called FindRoot to Eq.(17) with the experimental value of x_2 and to Eq.(18) with the experimental value of x_1 (see Fig. 7(a)), since Eqs.(17) and (18) are complicated functions of k . In Fig. 8(a) we show the value of k as a function of d thus obtained. The value of k drastically decreases with increasing d . The value of k is a little larger than those obtained from the first method at the same d . The least-squares fit of the data of k vs d to Eq.(22) yields the parameters $\zeta = 57.1 \pm 6.9$ and $n = 2.48 \pm 0.05$ for x_1 and $\zeta = 149 \pm 33$ and $n = 2.92 \pm 0.09$ for x_2 . The latter result is in excellent agreement with the prediction ($\zeta = 151.5$ and $n = 3.0$). In spite of such different values of ζ , it may be concluded experimentally that two magnetic moments made from coils are coupled through the dipole-dipole interaction with the exponent n being equal to 3.

Finally we discuss the effect of the asymmetric configuration on the trajectory in the (μ, ν) plane. As shown in Fig. 6, the trajectory rotates clockwise compared to the case of the trajectory in the symmetric configuration. Figure 9(a) shows the simulation plot of the μ as a function of x for the asymmetric configuration ($L_1 = 0.8201$ H and $L_2 = 0.8215$ H) as k is changed as a parameter, where $Q = 151.5$. Double peaks of μ around $x = 1$ is not symmetric with respect to $x = 1$. The peak at the high- x side is higher than that at the low- x side. Double peaks become closer and closer as k is decreased. Figure 9(b) shows the simulation plot of the trajectory in the (μ, ν) plane under the same condition as Fig. 9(a). The trajectory rotates counterclockwise compared to the case of the trajectory in the symmetric configuration. Figures 10(a) and (b) show the simulation plot of μ as a function of x and the trajectory in the (μ, ν) plane for the asymmetric configuration ($L_1 = 0.8201$ H and $L_2 = 0.8198$ H), where $Q = 151.5$ and k is changed as a parameter. Double peaks of μ around $x = 1$ is not symmetric with respect to $x = 1$. The peak at the high- x side is lower than that at the low- x side. The trajectory rotates clockwise compared to the case of the trajectory in the symmetric configuration. These features are in good agreement with those observed in the present measurement (see Fig. 5(a) for the μ vs x curve and Fig. 6 for the trajectory). So we can conclude that L_1 is a little larger than L_2 , which means the asymmetric configuration for the present measurement.

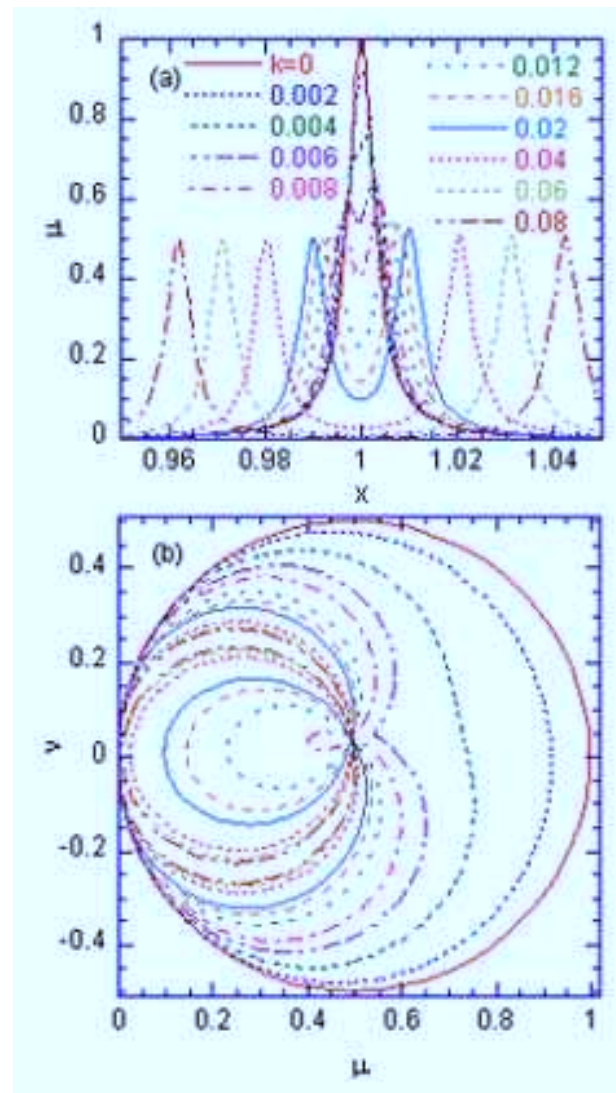


FIG. 9: (Color online) (a) Simulation plot of the real part (μ) as a function of x , where $Q = 151.5$ and $L_1 = 0.8207$ H and $L_2 = 0.8215$ H (the asymmetric configuration). (b) The trajectory of the point (μ, ν) for $Q = 151.5$, $L_1 = 0.8207$ H and $L_2 = 0.8215$ H (the asymmetric configuration), when x is varied from $x = 0$ to 3. The coupling constant k is changes as a parameter: $k = 0 - 0.1$.

VI. COCLUSION

We present a simple method for determining the mutual inductance of the AC coupled circuit using a digital dual-phase lock-in amplifier. This method allows one to get a large amount of data on the frequency dependence of the real and imaginary part of the AC output voltage in a reasonably short time. Our experimental results show that the coupling constant of the two coils is proportional to d^{-n} with an exponent n (≈ 3), where d is the distance between the centers of coils. When the current flows in the coils, the coil is magnetically regarded as the magnetic moment. So the physics of the mutual induc-

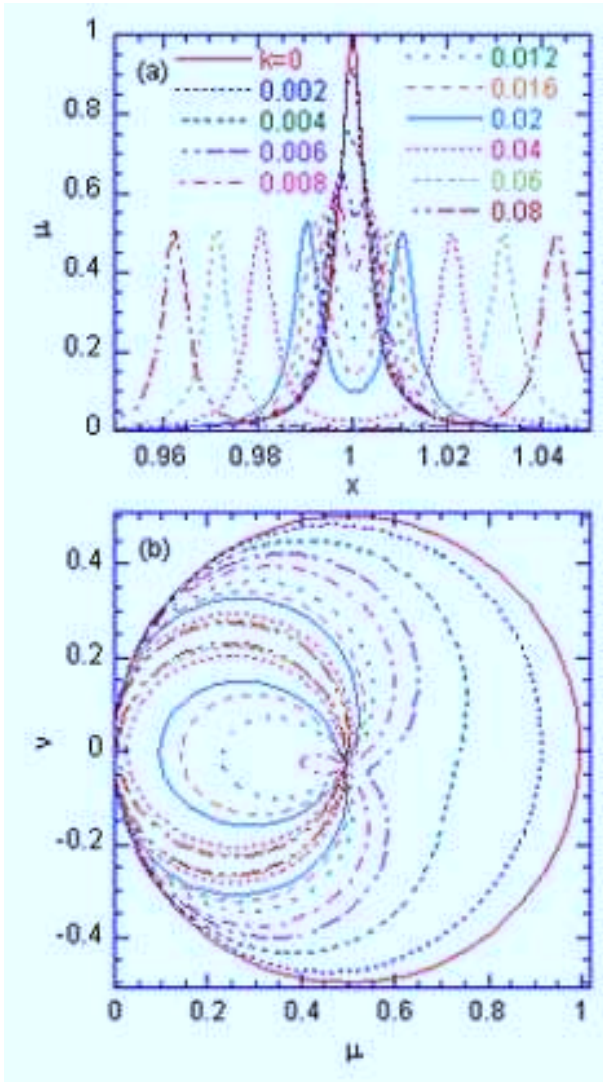


FIG. 10: (Color online) (a) Simulation plot of the real part (μ) as a function of x , where $Q = 151.5$ and $L_1 = 0.8207$ H and $L_2 = 0.8198$ H (the asymmetrical configuration). The coupling constant k is changed as a parameter: $k = 0 - 0.1$. (b) Typical trajectory denoted by the point (μ, ν) for $Q = 151.5$ (the asymmetric configuration), when x is varied from $x = 0$ to 8. The coupling constant k is changes as a parameter: $k = 0 - 0.1$.

tance is similar to that of two magnetic moments coupled each other. We find that the interaction between these two magnetic moments is a dipole-dipole interaction.

Acknowledgments

We are grateful to Mark Stephens for providing us with two coils with almost symmetric shapes.

* itsuko@binghamton.edu

† suzuki@binghamton.edu

¹ J.D. Jackson, *Classical Electrodynamics*, Second edition (John Wiley & Sons, New York, 1975).

² Stanford Research System, SR850 Instruction Manual.

³ H. Nagaoka, J. Coil Sci. Tokyo **27**, 18 (1909).

⁴ A.B. Pippard, *The Physics of vibration volume 1, containing Part 1, The simple classical vibrator* (Cambridge University Press, Cambridge, 1978).